Biogeosciences Discuss., 10, 17893–17937, 2013
www.biogeosciences-discuss.net/10/17893/2013/
doi:10.5194/bgd-10-17893-2013

Biogeosciences
Discussions
Open Access

A novel reflectance-based model for evaluating chlorophyll concentration of fresh and water-stressed leaves

C. Lin[1], S. C. Popescu[2], S. C. Huang[1], Y. C. Chen[1], P. T. Chang[3], and H. L. Wen[1]

[1]Department of Forestry and Natural Resources, National Chiayi University, Taiwan
[2]Department of Ecosystem Science and Management, Texas A&M University, College Station, Texas, USA
[3]Department of Horticultural Science, National Chiayi University, Taiwan

Received: 21 August 2013 – Accepted: 26 October 2013 – Published: 18 November 2013

Correspondence to: C. Lin (chinsu@mail.ncyu.edu.tw)

Published by Copernicus Publications on behalf of the European Geosciences Union.

Abstract

Water deficit can cause chlorophyll degradation which decreases foliar chlorophyll concentration (Chls). Few studies investigated the effectiveness of spectral indices under water stress conditions. Chlorophyll meters have been extensively used for a wide variety of leaf chlorophyll and nitrogen estimations. Since a chlorophyll meter works based on the sensing of leaves absorptance and transmittance, the reading of chlorophyll concentration will be affected by changes in transmittance as if there is a water deficit in leaves. The overall objective of this paper was to develop a novel and reliable reflectance-based model for estimating Chls of fresh and water stressed leaves using the reflectance at the absorption bands of chlorophyll *a* and *b* and the red edge spectrum.

Three independent experiments were designed to collect data from three leaf sample sets for the construction and validation of Chls estimation models. First, a reflectance experiment was conducted to collect foliar Chls and reflectance of leaves with varying water stress using the ASD FieldSpec spectroradiometer. Second, a chlorophyll meter (SPAD-502) experiment was carried out to collect foliar Chls and meter reading. These two datasets were separately used for developing reflectance-based or absorptance-based Chls estimation models using linear and nonlinear regression analysis. Suitable models were suggested mainly based on the coefficient of determination (R^2). Finally, an experiment was conducted to collect the third dataset for the validation of Chls models using the root mean squared error (RMSE) and the mean absolute error (MAE). In all of the experiments, the observations (real values) of the foliar Chls were extracted from acetone solution and determined by using a Hitachi U-2000 spectrophotometer.

The spectral indices in the form of reflectance ratio/difference/slope derived from the chl *b* absorption bands (ρ_{645} and ρ_{455}) provided Chls estimates with RMSE around 0.40–0.55 $\mathrm{mg\,g^{-1}}$ for both fresh and water-stressed samples. We improved Chls prediction accuracy by incorporating the reflectance at red edge position (ρ_{REP}) in regression models. An effective chlorophyll indicator with the form of $(\rho_{645}–\rho_{455})/\rho_{REP}$ proved to

be the most accurate and stable predictor for foliar Chls concentration. This model was derived with an R^2 of 0.90 ($P < 0.01$) from the training samples and evaluated with RMSE 0.35 and 0.38 $mg\,g^{-1}$ for the validation samples of fresh and water stressed leaves, respectively. The average prediction error was within 14 % of the mean absolute error.

1 Introduction

Photosynthesis is the largest-scale synthetic process on earth. There are many kinds of photosynthetic pigments, i.e., chlorophylls, carotenoids and phycobilins in plant leaves, but chlorophylls are considered to be the key factor because the photochemical reactions take place only at the trap chlorophyll molecules. Light absorbed by chlorophyll excites electrons in the molecules, enabling them to be transferred to other molecules for glucose production and thus enabling vegetation growth. Chlorophyll content can directly determine photosynthetic potential and primary production (e.g., Whittaker and Marks, 1975). About 100 billion tons of carbon could be fixed annually into organic compounds by photosynthetic organisms (Nobel, 2005). The forest, a union ecosystem of numerous trees, shrubs, savanna and lichens, uptakes carbons for vegetation metabolism and thus it makes a positive net primary production of biomass carbon.

Foliar chlorophylls concentration (shortened as Chls) has always been one of the important issues of research using vegetation remote sensing techniques in last two decades. As a consequence, a number of spectral indices were developed for foliar Chls estimation. Table 1 lists some of the chlorophyll indicators that have been examined by Vogelmann et al. (1993), Elvidge and Chen (1995), Blackburn and Ferwerda (2008), Ustin et al. (2009), Féret et al. (2011), and Hunt et al. (2013). Those indices integrate a couple of specific signatures of visible and near-infrared bands, for example, the reflectance at 445, 550, 680, 700, 705, 710, 720, 750, 780, 800, 860 nm for foliar Chls estimation.

Typical reflectance of vegetation in the visible-infrared region will level up as water deficit occurs (Knipling, 1970; Gausman and Allen, 1973; Gausman et al., 1982; Hunt and Rock, 1989; Carter, 1991 and 1993; Ceccato et al., 2001; Zygielbaum et al., 2009; Lin et al., 2012). As leaves dehydrate or vegetation is suffering water stress, leaf water potential becomes increasingly negative and the rate of photosynthesis is reduced (Nilsen and Orcutt, 1996; Montagu and Woo, 1999; Keenan et al., 2009; Lavoir et al., 2009) because water deficit can cause chlorophyll degradation and thus significantly decreases foliar chlorophyll concentration (Kirnak et al., 2001; Pirzad et al., 2011; Desotgiu et al., 2012; Ghorbanli et al., 2013). Specifically, the magnesium ion (Mg^{2+}) of the chlorophyll will be removed. As a result, chlorophyll becomes pheophytin (chlorophyll without Mg^{2+}) and inactivates the photochemical reaction (Kaoau et al., 2007; Schelbert et al., 2009; Weber et al., 2009); furthermore leaves decrease the absorptance of blue and red light while increase the reflectance at the corresponding wavelength bands. This underpins the first basic assumption of this study, that a spectral index that effectively integrates the reflectance at the blue and red bands, at which the light specifically absorbed by chlorophyll is only used for plant photosynthesis, is better for foliar Chls estimation than the indices (listed in Table 1) that use other than the blue and red bands.

The dynamics of pigment concentrations are diagnostic of a range of plant physiological properties and processes (Blackburn, 2007). A suitable chlorophyll index can offer useful information for estimating the gross productivity of terrestrial ecosystem (Nave et al., 2011) and even for understanding the dust storm events (Tan et al., 2011). In order to address the effects of global climate changes, it is necessary to continuously update the prediction of forest carbon sequestration and the net primary productivity of terrestrial ecosystem. Traditional methods of using spectrophotometer and/or fluorometer in destructively ground leaf liquids operate on the light absorption of leaf in a laboratory setting. Foliar Chls determined by this technique is practically used as a standard measurement for applications. Chlorophyll meter offers a fast and convenient alternative of foliar Chls measurement in recent years. The Minolta SPAD 502 is wildly used for a wide variety of leaf chlorophyll and nitrogen estimation by measuring the amount of light transmittance and absorptance in an easy and nondestructive way (Takebe et al., 1990; Ma et al., 1995; Blackmer and Schepers, 1995; Cate and Perkins, 2003; Read et al., 2003; Rowland et al., 2004; Hawkins et al., 2009; Rascher et al., 2009; Boegh et al., 2012). Nevertheless, it will be an extremely hard work to extend the result of traditional methods to field study because such single leaf measurement will be helpless (due to no connection) for up-scaling the Chls and/or the fraction of absorbed photosynthetically active radiation (Gond et al., 1999) for the levels at tree crown or stand canopy.

In addition, since a chlorophyll meter works based on the sensing of leaves absorptance and transmittance, the reading of chlorophyll concentration will be affected by changes in transmittance as if there is a water deficit in leaves. On the other hand, the use of the relationship between the chlorophyll concentration and the readings of the chlorophyll meter is possibly may not accurately observe the chlorophyll variations due to physiological stresses. While remote sensing only uses the reflectance to differentiate materials and/or discern the properties of targets, it therefore can offer good opportunity to indirectly determine foliar Chls. Therefore, the second assumption of this study is based on the fact that foliar reflectance at the photosynthesis wavebands is a better representative of foliar biochemical spectra than single leaf transmittance (hand-held chlorophyll meter) in nondestructive detection base.

Many researches indicated that the spectral characteristics of red edge (RE) and green peak (GP) are directly or indirectly correlated to the level of leaf chlorophyll (Horler et al., 1983; Curran et al., 1990; Filella and Peñuelas, 1994; Pinar and Curran, 1996; Jongschaap and Booij, 2004; Mutanga and Skidmore, 2007) and can provide a method to distinguish between water and nutrient stress (Estep and Carter, 2005), they should be helpful in the prediction of leaf chlorophyll concentration. However, few researches examined the effectiveness of remote sensing models in the estimation chlorophyll content of both fresh and water stressed leaves. We therefore proposed as a major goal of our study to develop a spectral index which could effectively integrate the reflectance of the photosynthetic related spectra for leaf chlorophyll determination in a reliable nondestructive way for field application.

Briefly, the null hypotheses specified as follow will be examined in this paper.

H01: The reflectance at the wavelengths (e.g., 663 nm, 645 nm, 455 nm, and 426 nm, shortly ChlsPn variables) directly absorbed by chlorophyll for photosynthesis is significantly and negatively related to foliar Chls with respect to variation of leaf water content.

H02: Reflectance-based spectral indices derived from ChlsPn/RE/GP variables are closely related to foliar Chls and can make better estimations of Chls than other indices without ChlsPn variables in respect to different degree of water stress situations.

H03: The determination of foliar Chls using the transmittance-based meter (e.g. SPAD chlorophyll meter) is insensitive to leaf water content.

2 Materials and methods

There were two independent experiments adopted to develop the foliar chlorophyll concentration models. The first was the chlorophyll-reflectance experiment from which training leaf samples were collected for reflectance measurement and chlorophyll determination, and the second was the chlorophyll-SPAD experiment in which a new set of leaf samples was collected independently for SPAD measurement and chlorophyll concentration determination. Finally, additional leaf samples were used as test dataset for further validation of those models developed based on foliar reflectance experiment or SPAD absorptance experiment.

A hardwood species, namely Camphor tree (*Cinnamomum camphora* (Linn.) Seib), was selected for experiments. Leaf samples with size around 6–8 cm long by 3–4 cm wide were collected from the campus of National Chiayi University in Taiwan. The authors intended to have samples collected in a wide range of pigment concentration to meet the needs of this study. According to the ground inventory, we collected samples to meet leaf colors from dark green, light green, yellowish green, red, to dark red for laboratory experiments. Leaf samples of the datasets for chlorophyll-reflectance exper-

BGD
10, 17893–17937, 2013

iment and chlorophyll-SPAD experiment is 50 and 45 respectively, and the additional evaluation dataset is 70 leaves.

2.1 Data acquisition

2.1.1 Determination of foliar chlorophyll contents

Wellburn (1994) demonstrated that the pigment of leaf pigments could be determined by acetone, chloroform, dimethyl-formamide, and dimethyl-sulphoxide with spectrophotometer analysis. Concentrations of the tested foliar chlorophylls were extracted from the 80 % acetone solution and determined spectrophotometrically using a Hitachi U-2000 spectrophotometer following the method of Arnon (1949). Concentration of chlorophyll *a* (chl *a*) and chlorophyll *b* (chl *b*) are determined using Eqs. (1) and (2) where D_λ stands for the absorptance at the specific wavelength λ, V and W represent the volume of ground leaf-acetone liquid (mL) and the fresh weight (g) of the ground leaf, respectively. Total chlorophylls concentration, Chls, was expressed as milligrams of chlorophyll per gram of fresh leaf weight ($\mathrm{mg\,g^{-1}}$) and can be derived by summing up the values of chl *a* and chl *b*.

$$\mathrm{Chl}\ a = (12.7 \times D_{663} - 2.69 \times D_{645}) \times (V/1000\,\mathrm{W}) \qquad (1)$$

$$\mathrm{Chl}\ b = (22.9 \times D_{645} - 4.68 \times D_{663}) \times (V/1000\,\mathrm{W}) \qquad (2)$$

2.1.2 Foliar reflectance measurement

Spectral data were obtained from the FieldSpec Pro FR spectroradiometer manufactured by Analytical Spectral Devices (ASD). This instrument measures spectra over a spectral range of 350–2500 nm and offers 1 nm-wide narrowband spectral data. Specifically, the FWHM spectral resolution of the FieldSpec Pro FR spectroradiometer is 3 nm for the region 350–1000 nm and 10 nm for the region 1000–2500 nm (Hatchell, 1999) which meets the nominal sampling and resolution requirements for hyperspectral remote sensing applications (Curtiss and Goetz, 1994).

Procedures to gathering spectra involves optimizing the integration time (typically set at 17 ms), providing foreoptic information, recording dark current, collecting spectralon reference radiance, and then obtaining target radiance. A 25° field of view (FOV) foreoptic which connected ASD spectroradiometer and the computer control system was mounted 35 cm above and leveled at a tripod on the top of leaf samples. As a result, a pixel size of 1.5 cm was determined as optimal. A black cloth was used to cover the platform to avoid the influence of background reflection. Two light sources were face to face mounted at an elevation angle of 45° and 1 m away from the sample. The target reflectance is determined as the ratio of the energy reflected off the target (target radiance) to energy incident on the reference spectralon (reference radiance). For each measurement, the radiance was taken with spectrum averaging set to 15 and then filtered using a median filter (Hatchell, 1999; Lin et al., 2012).

Leaves reflectance spectra were measured in a laboratory with an artificial illuminator (USHIO jc 14.5V-50WC) supported light energy before the leaves grinding process for chlorophylls determination. The ASD spectroradiometer collects one nanometer resolution hyperspectral data. A first derivative transformation of the reflectance spectra (Dawson et al., 1998) was applied to calculate the slope values (FDS) of the foliar reflectance spectra and to determine the red edge position. This position has the largest FDS value which indicates the maximum change in the slope of the reflectance spectra per unit change in wavelength. Red edge position generally moves toward the longer wavelength if the FDS become larger which is as a result of high chlorophylls concentration in leaf. Leaf color is generally applied to visually diagnose foliar chlorophyll or healthy status. Green peak is supposed to be the main syndrome of foliar greenness and probably could offer potential value in the foliar Chls estimation. Green peak position is determined if the FDS value equals to zero.

2.1.3 Implement of spectral and chlorophyll measurement of fresh and water-stressed leaves

Relative water content (RWC) of leaves is commonly used to assess the water status of plants in tree physiology researches. It has been applied to describe the status of leaf water-stress in remote sensing (Pu et al., 2003; Lin et al., 2012) and is therefore used in this study. Fresh leaf samples were first detached, measured for fresh weight (FW), and then spectral reflectance data were immediately collected. Leaf samples were then left to dry naturally in an air-conditioned room at 26 °C with circulated air by fan. Measurements of leaf weight and reflectance were made every two hours during the drying process for 24 h. After collecting the final drying leaf weight and spectra, the leaf samples were oven-dried and the absolute dry weight (WD) was recorded. Finally, the RWC of fresh leafs and drying leafs were determined using Eq. (3). We further refer to this experiment as the pilot experiment.

$$\mathrm{RWC} = \frac{\mathrm{FW} - \mathrm{WD}}{\mathrm{FW}} \times 100 \tag{3}$$

The first experiment is chlorophylls-reflectance experiment in which total 50 leaves were first used for spectral measurement and then ground for chlorophyll concentration determination. The second experiment is the chlorophylls-SPAD experiment which was designed for exploring the relationship of the SPAD readings and leaf chlorophyll contents. A chlorophyll meter SPAD-502 (Konica Minolta Sensing, Inc) was used for quick measurements of the chlorophyll content. In this experiment, we had 45 samples which were first measured by SPAD readings then ground and dissolved in acetone solution for chlorophyll concentration determination. Data collected from these two experiments were used for correlation and regression analysis to derive the relationships of Chls-reflectance spectra and Chls-SPAD readings. The third experiment is a validation experiment. Additional 70 leaf samples were first detached and measurements of their weight were recorded along with SPAD and reflectance of fresh leaves, and then left to dry naturally in the same environment conditions as the pilot experiment.

BGD
10, 17893–17937, 2013

24 h later, spectral measurements were implemented immediately after obtaining the weight and SPAD measurements for every leaf samples. A small portion, a circle with a diameter of 1.5 cm, (set W_s) of each of the leaf samples (set W_{total}) was taken for the determination of foliar Chls in the acetone solution, and the another part of each of the leaf samples was oven-dried to get the dry weight for the determination of leaf RWC based on the weight ratio of W_s and W_{total}.

2.2 Correlation analysis and regression analysis

A correlation analysis was applied to determine the correlation coefficient (r) between the foliar chlorophylls concentration and its reflectance. All of the coefficients were further tested using the Student's t statistic $t = r\sqrt{(n-2)/(1-r^2)} \sim t_{\alpha/2,n-2}$ to examine whether it is statistical meaningful for diagnosing foliar chlorophylls status.

Arnon (1949) demonstrated that chlorophyll *a* and chlorophyll *b* have their particular absorption features in the blue and red spectral region in the acetone solution. Specifically, chl *a* and chl *b* have two absorption peaks for photosynthesis at the wavelength of 426 nm and 663 nm, and 455 nm and 645 nm, respectively. The absorption peaks of chl *a* and chl *b* in other solvents, such as chloroform, shift a little from the predefined wavelength (Wellburn, 1994). Since the chlorophyll was determined by using the acetone solvent, the spectral reflectance at those four specific wavelengths, i.e., ρ_{663}, ρ_{645}, ρ_{445}, and ρ_{426} are called ChlsPn variables; the chlorophyll related spectra such as the position and reflectance of the green peak feature (λ_{Gmax} and ρ_{Gmax}) and the red edge feature (λ_{REP} and ρ_{REP}) are called GP variables and RE variables. A transformation of two key spectral features can be integrated by simple ratio (ρ_i/ρ_j), simple difference ($\rho_i - \rho_j$), and normalized difference $(\rho_i - \rho_j)/(\rho_i + \rho_j)$ methods to derive a new spectral index for remote sensing analysis. A new transformation, the slope index (SI), was defined as the ratio of the spectral difference and the distance of any two key features. That is $\mathrm{SI} = (\rho_i - \rho_j)/(|\lambda_i - \lambda_j|)$. This index integrates two spectral reflectance values based on their spectral curve (or spectral behavior) into a standardized

BGD
10, 17893–17937, 2013
Effective chlorophyll indicators for fresh and water-stressed leaves
C. Lin et al.

index value and potentially can reduce the influence caused by background and various albedo. The original form of the variables ChlsPn, GP, and RE and their derived spectral indices (Eqs. 6–21) were used as variables (shown in Table 2) in regression analysis. Reflectance-based empirical Chls models were than validated to examine the hypotheses of this study.

In the regression analysis of reflectance-based models, the dependent variable is the natural logarithm transformed foliar Chls, denoted as lnChls. The transformation is used to stabilize the constant variance of the predicted error term. And the independent variable is the ChlsPn variables, the GP variables, the RE variables, and/or their derived spectral indices. The statistics such as the coefficient of determination (R^2), the prediction error sum of squares (PRESS), and the standard error of estimates (SE(Y)) were used to measure the model adequacy. In the regression analysis of SPAD-based chlorophyll model, the SPAD-readings and acetone-extracted chlorophyll was set to be the regressor variable and the dependent variable, respectively; the fitted model is named as absorptance-based chlorophyll model.

2.3 Validation of reflectance-based and absorptance-based chlorophyll empirical models

The reflectance spectra and SPAD readings collected by the third experiment were input to the absorptance-based model and the reflectance-based models to get the estimates of the foliar chlorophylls concentration; and each of the estimates was then assessed by the acetone-method determined chlorophylls contents. In the prediction assessment, the formula of root mean squared error (RMSE) and mean absolute error (MAE) are listed in Eqs. (4) and (5) and applied to demonstrate how the estimator differs from the measured value of the quantity being estimated. RMSE has the same units ($\mathrm{mg\,g^{-1}}$) as the quantity being estimated, and MAE is presented in percentage indicating a relative degree of the estimation differs from the observation. In Eqs. (4) and (5), n is the number of samples, y and $\hat{y}$ represents the observed and predicted

BGD
10, 17893–17937, 2013

value respectively.

$$\mathrm{RMSE} = \sqrt{\frac{\sum_{i=1}^{n}(y_i - \hat{y}_i)^2}{n}} \tag{4}$$

$$\mathrm{MAE} = \frac{1}{n}\left[\sum_{i=1}^{n}\frac{\mathrm{abs}(y_i - \hat{y}_i)}{y_i} \times 100\,\%\right] \tag{5}$$

3 Results

3.1 Reflectance spectra of fresh and water-stressed leaf

Figure 1a shows the spectral behavior of the fresh and water-stressed leafs of camphor trees. RWC of the leaf sample varied from 51 % to 5 %. Four aspects could be pointed out about the difference of reflectance spectra between fresh and water-stressed leafs. First, reflectance spectra in the visible-infrared region behaved like a general reflectance curve of fresh green leaves while the curve lifts up as the RWC decreased. Second, the green peak of the reflectance curves was always clearly visible and the slope from the peak at green region to the lowest point at red region was significantly decreased when RWC is less than 30 %. Third, the significant water absorption valleys could be seen at the spectral regions centered at 1450 and 1910 nm. The depth and the area of the absorption valley are negatively close related to leaf RWC (Lin et al., 2012). Finally, a water-stressed leaf reflectance peaked at around 2000 nm as the RWC less than or equal to 16 %. Although the absorption feature in the infrared region (2000–2200 nm) is possibly due to the dry matter constituents (such as protein, lignin and cellulose) (Cheng et al., 2011), this particular phenomenon is probably related to physiological reactivity. It should be worthy to explore in further studies. Figure 1b shows the first derivative of reflectance in the visible region of a sample leaf.

The red edge and green peak of the sample leaf were detected at around 701–697 nm and 540–535 nm, respectively. It was observed that a small shift from longer to shorter wavelength happened as RWC changed from 51 % to 5 %. Even though the shifts were not very significant, it still indicated that the foliar Chls would decrease if the water content of leaves decreased. This phenomenon agree with the one addressed by Kirnak et al. (2001), Pirzad et al. (2011), Desotgiu et al. (2012) and Ghorbanli et al. (2013).

3.2 Response of leaf reflectance to variations in leaf chlorophyll concentration

Figure 2a demonstrates the reflectance spectra over the visible-infrared wavebands of the fresh leaves in the experiment one. The Chls of these samples ranged from 0.7 to 4.1 $mg\,g^{-1}$. An important feature that was observed showed that the change of reflectance in the visible region behaves obviously different from the one in the infrared region due to changes of foliar Chls. Leaf with smaller Chls showed a higher reflectance in the visible portion of the spectrum. This is very similar to the level-up of the reflectance curve as leafs are in a water stress situation. But, on the contrary, a leaf with higher Chls demonstrated a higher reflectance in the infrared area, while the reflectance levels up in the infrared region, which is not always consistent with the increase of foliar Chls among all of the samples.

The blue drop and the red drop in the visible region are due to photons being absorbed by the chlorophylls *a* and *b* in the photosynthesis process (Emerson and Lewis, 1943; Hopkins and Hüner, 2004). It indicates that a sharp decrease happened to the gradient between these two points (shortly gradient) for the leaf with higher value of Chls. On the other words, a leaf whose reflectance in visible region will level down and the gradient will also decline as it is getting mature. Associations between the green peak and the red edge features and values of foliar Chls are shown in Fig. 2b, which indicates that the green peaks and the red edge occur at wavelengths around 554–557 nm and 694–715 nm, respectively. As foliar Chls decreased, the red edge position moves toward shorter wavelengths, the same trend being observed for the blue edge.

BGD
10, 17893–17937, 2013

3.3 Relationship of chlorophylls concentration and visible-infrared reflectance spectra

Leaf spectral reflectance (ρ_λ) is correlated to foliar Chls. Figure 3 demonstrates the generalized visible-infrared spectra of *Cinnamomum camphora* leaves and associated with the corresponding correlogram of Pearson's correlation coefficients, denoted as $r(\text{Chls}, \rho_\lambda)$ a correlation coefficient of the foliar chlorophyll concentration and the reflectance at wavelength λ. A negative coefficient $r(\text{Chls}, \rho_\lambda) < 0$ was found in the visible region while a positive coefficient $r(\text{Chls}, \rho_\lambda) > 0$ was found in the infrared region.

Most of the reflectance values between 350–2500 nm have proven to be significantly linearly related to foliar Chls based on the Student's t statistic $t = r\sqrt{(n-2)/(1-r^2)} \sim t_{\alpha/2,n-2}$. Exceptions are the sub-regions 730–741, 1905–1970, and 2408–2500 nm. Reflectance of the bands at green sub-region 530–580 nm and red edge sub-region 700–716 nm are valuable because absolute value of their $r(\text{Chls}, \rho_\lambda)$ are greater than 0.90 ($P < 0.01$). Although vegetation is proven to use the light energy in blue (PS I) and red (PS II) wavelength for photosynthesis, the reflectance spectra seem not identical to the absorption spectra.

Infrared reflectance is positively related to foliar Chls. It is noticed that in the first sub-region of shortwave infrared, a dramatic drop of reflectance curve happened in the water absorption area (1395–1504 nm, denoted as SWIR I), with a value of $r(\text{Chls}, \rho_\lambda)$ around 0.75. In the second sub-region of shortwave infrared (1905–1970 nm, denoted as SWIR II) the reflectance is almost independent of foliar Chls because the value of $r(\text{Chls}, \rho_\lambda)$ is almost identical to zero, as indicated by the Student's t test result.

BGD
10, 17893–17937, 2013

4 Discussions

4.1 Reflectance-based empirical models for the estimation of total chlorophyll content

4.1.1 Adequacy comparison among the models with prototype variables

Recall that a measured value of foliar chlorophyll is determined by the spectrophotometrical method. This method uses the absorptance peaks of blue spectra at 426 nm and 455 nm and the absorptance peaks of red spectra at 645 nm and 663 nm. The reflectance of those specific wavelengths, i.e., ρ_{426}, ρ_{455}, ρ_{645}, and ρ_{663} are named as the ChlsPn variables, the red edge characteristics ρ_{REP} and λ_{REP} are named as red edge variables and the green peak characteristics ρ_{Gmax} and λ_{Gmax} are named as green peak variables hereafter in this paper.

Based on the fundamentals of remote sensing, a target will reflect smaller amount of incident energy if it absorbs most of the incident energy. Figures 4a–d shows that foliar chlorophylls concentration is negatively related to the reflectance of the ChlsPn variables. It indicates that a higher foliar chlorophyll concentration causes a lower reflectance of the blue and red spectra. The models with one of the ChlsPn variables work like the spectrophotomerical method. Figure 4e and 4f show that the chlorophylls concentration is positively linearly related to the red edge variables indicating the result similar to Curran et al. (1991). The adequacy statistics R^2, PRESS, and SE(Y) show that λ_{REP} is better than ρ_{REP} and even better than ρ_{645} in the prediction of chlorophylls concentration. There are 89 % of the Chls variation could be explained by λ_{REP} while only 30 % of the Chls variation could be explained by ρ_{REP}. This result agrees with the research of Mutanga and Skidmore (2007) and Reddy and Matcha (2010) who demonstrated that the red edge position is strongly negatively correlated with the foliar pigment concentration in plants. The reductions in Chls increased leaf reflectance at red spectral region and caused the red edge shift to shorter wavelengths. This agrees with conclusions of Carter (1993) and Carter and Knapp (2001). Though the Chls of

BGD
10, 17893–17937, 2013

training samples show a big variation, the green peak position (λ_{Gmax}) changes only in a very short span from 554 to 557 nm. There is only 10 % of Chls that could be explained by the variable λ_{Gmax} (Fig. 4g). The Chls is much better fitted by the reflectance of the green peak position (ρ_{Gmax}) with a negatively linear relationship (Fig. 4h). This model has adequacy very close to the model with the regressor λ_{REP}.

4.1.2 Adequacy comparison among the models using a derived spectral index

Figure 5 shows the relationship between the lnChls and the difference index or the slope index of red and blue absorption peaks by the prototype variables, and of the green peak and red edge variables. RDI_a and SI_a are negatively linear related to lnChls while SI_a has a better model adequacy than RDI_a (Fig. 5a and b). This kind of adequacy variation was not observed with the other two pairs of predictors. It is observed that both predictors RDI_b and SI_b have an exponential decay relationship with the lnChls (Fig. 5c and d), the regression coefficient of the predictor is negative which means that a lower value of total chlorophyll concentration will be observed when having a higher value of RDI_b or SI_b. The model adequacy indicators of these two models are identical.

The predictors $RDI_{\rho_{REP}-\rho_{Gmax}}$ and $SI_{\rho_{REP}|\rho_{Gmax}}$ work like a two-order polynomial function in the prediction of lnChls. These two models also have same levels of the indicators of model adequacy (Fig. 5e and f). The coefficients of first- and second-order variables are negative indicating a higher value of foliar Chls has a lower value of $RDI_{\rho_{REP}-\rho_{Gmax}}$ and $SI_{\rho_{REP}|\rho_{Gmax}}$. In other words, a leaf with high chlorophyll concentration will have the reflectance at the red edge position far greater than the reflectance at the green peak position. Based on the value of R^2, it is suggested that the spectral indices derived from the chlorophyll *b* absorption features (RDI_b and SI_b) are better than the other four indices from chlorophyll *a* absorption features or green peak and red edge features.

Figure 6 shows six empirical models with adequacy assessments for the estimation of foliar chlorophylls concentration using the ratio index of spectral features. Those

BGD
10, 17893–17937, 2013

models are all negatively related to the lnChls. The lnChls has a linear relationship with the predictors RI_a, RI_b, $\mathrm{RI}_{\mathrm{SPAD}}$,

$\mathrm{RI}_{\rho_{\mathrm{Gmax}}/\rho_{\mathrm{REP}}}$, and $\mathrm{RI}_{\mathrm{RDI}_b/\rho_{\mathrm{REP}}}$ (Fig. 6a–e), while it has an exponential relationship with the predictor $\mathrm{RI}_{\mathrm{RDI}_b/\lambda_{\mathrm{REP}}}$ (Fig. 6f). We found that the RDI_b spectral features in the prediction of lnChls could be retained by $\mathrm{RI}_{\mathrm{RDI}_b/\lambda_{\mathrm{REP}}}$ when RDI_b is constrained to the behavior of λ_{REP} simultaneously while this is not observed for the $\mathrm{RI}_{\mathrm{RDI}_b/\rho_{\mathrm{REP}}}$. The R^2 of those models in explaining lnChls variation with ratio index regressor is between 0.66 and 0.93 ($P < 0.01$). It is suggested that the predictors $\mathrm{RI}_{\rho_{\mathrm{Gmax}}/\rho_{\mathrm{REP}}}$, $\mathrm{RI}_{\mathrm{RDI}_b/\rho_{\mathrm{REP}}}$, and $\mathrm{RI}_{\mathrm{RDI}_b/\lambda_{\mathrm{REP}}}$ are better than RI_a, RI_b, $\mathrm{RI}_{\mathrm{SPAD}}$.

Figure 7 shows the behavior of normalized difference indices with respect to the changes of foliar total chlorophylls concentration. The predictors NDI_a and NDI_b are linearly related to lnChls (Fig. 7a and b). These two indices display a negative relationship in the estimation of lnChls, with an R^2 value of 0.67 and 0.83 ($P < 0.01$). $\mathrm{NDI}_{\mathrm{REPRDIb}}$ is positively and linearly related to changes of lnChls (Fig. 7c), while $\mathrm{NDI}_{\mathrm{REPGmax}}$ is nonlinearly related to the changes of lnChls (Fig. 7d). Their R^2 values are 0.91 and 0.93 ($P < 0.01$). The adequacy of the latter two NDI models is better than the former two NDI models.

4.1.3 Validation of empirical reflectance-based Chls models

The empirical reflectance-based Chls models developed using the training samples were validated using another data set, by using samples which contains fresh and water stressed leaves. The Chls prediction bias was presented with the indicators RMSE and MAE in response to the group of fresh and water stressed samples, shortly RMSEf and RMSEw and MAEf and MAEw. The prediction bias of both fresh and water stressed groups was averaged to get the mean values of RMSEa and MAEa. Detail of the model validation and percent variances explained are listed in Table 3. Among the 24 models, there are 11 models whose R^2 is greater than 0.90 ($P < 0.01$), PRESS is less than 1.60, and SE(Y) is less than 0.25. Though those models have high R^2 values,

BGD
10, 17893–17937, 2013

the predicted Chls accuracy for the validation data set varies significantly. Some of the models have a big difference in prediction power for fresh leaves and water stressed leaves samples. For examples, the model with the predictor $\mathrm{RDI}_{\rho_\mathrm{REP}-\rho_\mathrm{Gmax}}$, $\mathrm{SI}_{\rho_\mathrm{REP}|\rho_\mathrm{Gmax}}$, or λ_REP has MAEs for fresh and water stressed leaves greater than 50 % and 39 %; the model with the predictor $\mathrm{RI}_{\rho_\mathrm{Gmax}/\rho_\mathrm{REP}}$ or $\mathrm{NDI}_\mathrm{REPGmax}$) has MAEs for fresh leaves under 17 % but for water stressed leaves values are over 89 %; the model with the predictor ρ_Gmax has MAE greater than 44 % and 140 % for fresh leaves and water stressed leaves, respectively. These results indicate that $\mathrm{RI}_{\rho_\mathrm{Gmax}/\rho_\mathrm{REP}}$ and $\mathrm{NDI}_{\rho_\mathrm{REPGmax}}$ models are only recommended for the Chls estimation of fresh leaves, while they failed to capture the changes caused by the water stressed effect on spectral features variations.

Five models among those 24 models could be applied to estimate the foliar Chls of tree leaves because their predictor is able to capture accurately the Chls variation due to the changes of water content in leaves. The relatively high performance models have MAEs ranges between 15–20 % and 12–19 % for fresh leaves and water stressed leaves, and have average MAEs between 14 % and 18 %. Those models include the predictor $\mathrm{RI}_{\mathrm{RDI}_b/\rho_\mathrm{REP}}$, SI_b, $\mathrm{RI}_{\mathrm{RDI}_b/\lambda_\mathrm{REP}}$, RDI_b, or $\mathrm{NDI}_{\mathrm{REPRDI}b}$). It is found that the major spectral features are the reflectance difference index or slope index derived from the chl *b* absorptance bands, ρ_{645} and ρ_{455}. Briefly, the best validation among those reflectance-based Chls models was observed for the model with the predictor $\mathrm{RI}_{\mathrm{RDI}_b/\rho_\mathrm{REP}}$. Accordingly, we inferred the reflectance variables ρ_{645}, ρ_{455}, andρ_REP are able to capture the key spectral features of foliar chlorophyll status and hence bring an effective prediction of foliar Chls. Using $\mathrm{RI}_{\mathrm{RDI}_b/\rho_\mathrm{REP}}$ as a predictor, the Chls could be estimated with a prediction bias less than RMSEf 0.35 $\mathrm{mg\,g^{-1}}$ and RMSEw 0.38 $\mathrm{mg\,g^{-1}}$ for fresh and water stressed leaves. In addition, λ_REP could be an alternative spectral feature of ρ_REP to substitute it in the ratio index form of $\mathrm{RI}_{\mathrm{RDI}_b/\lambda_\mathrm{REP}}$. The Chls estimation bias is less than RMSEf 0.46 $\mathrm{mg\,g^{-1}}$ and RMSEw 0.42 $\mathrm{mg\,g^{-1}}$ for fresh leaves and water stressed leaves.

In addition, the model with only one reflectance feature of the prototype variables, i.e., ρ_{663}, ρ_{425}, ρ_{645}, or ρ_{455}, will not be able to successfully predict foliar Chls. Finally,

BGD
10, 17893–17937, 2013

we found that a confliction of agreement between model adequacy and validation for the models with the predictor λ_{REP} and ρ_{REP}. Though λ_{REP} is fitted very well with high adequacy $R^2 = 0.90$ ($P < 0.01$), its model is validated with MAEa = 52 % and RMSEa = 0.95 mg g^{-1}; while ρ_{REP} is not fitted very well, its $R^2 = 0.30$ is still significant at the 0.05 probability, and this model is validated with MAEa = 20 % and RMSE = 0.48 mg g^{-1}. The reflectance at green peak wavelength (ρ_{Gmax}) could be partially useful in the Chls prediction of fresh leaves.

Oki (2010) showed that ratio of reflectivity is able to have good estimation of chlorophyll *a* in lake water. Our results demonstrated that leaf chlorophyll concentration in cases of various water contents (fresh and/or water stressed) could be accurately predicted using spectral ratio indices such as RI (ratio index), SI (slope index), and NDI (normalized difference index) due to those indices can effectively integrate the spectral features of chlorophyll *b* and additionally the red edge characteristics. The model adequacy and the prediction accuracy validation of the empirical models have the same agreement. It leads to the answers of the hypotheses H01 and H02. First, the reflectance of ChlsPn is linearly and negatively related to foliar Chls, while the reflectance of red edge and green peak is linearly and positively related to foliar Chls. Second, the ChlsPn, red edge, and green peak cannot achieve an acceptable accuracy in the estimation of foliar Chls (for example MAE < 20 %) when they are used alone as predictors. Third, the ChlsPn variables can be integrated to produce a spectral difference index ($\mathrm{RDI}_b = \rho_{645} - \rho_{455}$) or a spectral slope index $\mathrm{SI}_b = (\rho_{645} - \rho_{455})/(\lambda_{645} - \lambda_{455})$ to achieve an acceptable accuracy. Finally, ChlsPn and red edge characteristics can also be integrated as new spectral indices by the combination of reflectance difference and simple ratio.

Specifically, foliar Chls is significantly related to the reflectance of ρ_{645} and ρ_{663} then ρ_{455} and ρ_{426}. But the spectral difference index (RDI_b) and the slope index (SI_b) work much better than each of the four variables. Moreover, the prediction accuracy of the spectral difference index can be further improved by 17 % if it is synergized with the reflectance at red edge position. That is an appropriate predictor and can be derived by $(\rho_{645}-\rho_{455})/\rho_{REP}$, denoted as $RI_{RDI_b/\rho_{REP}}$ in Table 2, for a better prediction accuracy of foliar Chls in respect to various foliar water contents.

4.1.4 A comparison with previously developed spectral indices of chlorophyll indicators

Relationships between lnChls and the previous 18 spectral indices in Table 1 were developed using the training samples. Mostly the lnChls (y in Table 4) is linearly and positively or negatively related to the indices, while an exponential decay relationship is observed between the lnChls and the indices TCI and SR_{775}. R^2 values for those models are mostly greater than 0.90, only the model with $NDVI_{680}$ has an R^2 of 0.60 showing a relatively poor model adequacy. Chls prediction accuracy of those models is between RMSE 0.87–4.57 $mg\,g^{-1}$ or MAE 39–177 % for both the fresh and water stressed leaves (Table 5). The best accuracy was achieved by the indicator $CI_{red\ edge}$ with an RMSE of 0.72 and 1.00 $mg\,g^{-1}$ and an MAE of 27 and 53 % for the fresh and water stressed validation samples. The foliar Chls is linearly and positively related to $CI_{red\ edge}$, as shown in Gitelson et al. (2009).

Although Ollinger (2011) suggested that the near-infrared region is the most important to vegetation remote sensing, a spectral index that combines the reflectance of near-infrared and red edge wavelengths was not able to achieve the same accuracy level of the predictor $RI_{RDI_b/\rho_{REP}}$. Specifically, taking the average of the prediction accuracy of both fresh and water stressed samples, the indicator $CI_{red\ edge}$ could achieve an accuracy of RMSE = 0.87 $mg\,g^{-1}$ and MAE = 39 %. That is almost 2.5 times of the average accuracy (RMSE = 0.36 $mg\,g^{-1}$ and MAE = 14 %) indicated by $RI_{RDI_b/\rho_{REP}}$. This is probably due to the structure of the foliar mesophyll which has changed when foliar water deficit happened. For example, Wuyts (2012) found that leaf thickness is conserved in response to water deficit under both high and low cumulative light regimes while mesophyll cells have changed in volume and shape. The change of the near-infrared

BGD
10, 17893–17937, 2013

reflectance is more complicated. Additional studies might be needed to explain the behavior of infrared reflectance in the future.

4.2 Evaluation of the absorptance-based Chls model (the SPAD-502 method)

4.2.1 Nonlinearity relationship between ln_transformed chlorophylls and SPAD readings

SPAD readings and total chlorophylls concentration relationship was explored from an independently experiment of 45 fresh leaf samples of *Cinnamomum camphora*. A 3-parameter rational function, $Y = (1 + aX)/(b + cX)$ was most appropriate for presenting the relationship of SPAD reading (X) and the lnChls (Y) based on the ANOVA F test of the fitted model and the t test of the model's parameters. Figure 8 showed that SPAD readings are nonlinearly dependent on the natural log-transformed Chls. Specifically, the coefficients, a, b, and c of this fitted model were further t tested to be significant at 0.01 level. Totally there 95.77 % of the variance of lnChls could be explained by the SPAD-Chlorophyll rational model. Compared with the measured value determined by the acetone-method, the fitted rational model has an average accuracy of 0.22 $mg\,g^{-1}$ RMSE and 15 % MAE that differ from the measured chlorophylls content for the training data set.

4.2.2 Limitation of the SPAD reading-based rational model

According to the experiment, we found that the SPAD reading increases positively in relationship to the chlorophyll concentration in fresh leaves. While the SPAD reading remained at a high value even when leaves are under serious water stress, that is the SPAD reading will raise to a high level even the chlorophylls content is decreasing. It revealed that the prelisted nonlinear rational model is not suitable for those wilting leaves. Figure 9 showed a shortage of SPAD reading-based model in the estimation of foliar chlorophylls content. The Chls estimates of fresh leaves (presented with black dots) mostly locate under the real Chls line (i.e., under estimation) and the Chls estimates of water stressed leaves (presented with circles) mainly locate above the real Chls line (i.e., over estimation). The biases RMSE and MAE of Chls estimation were evaluated to be $0.29\,\mathrm{mg\,g^{-1}}$ and 16 % for the fresh leaves sample and $0.92\,\mathrm{mg\,g^{-1}}$ and 60 % for the water stressed leaves sample. The fresh leaves sample has biases very close to the values (RMSE $0.22\,\mathrm{mg\,g^{-1}}$ and MAE 15 %) of the original modeling data set, but the water stressed leaves sample has biases almost four times that of the original modeling data set. It indicated that the SPAD rational model can achieve a very good and acceptable Chls estimates in case of fresh leaves, while unfortunately it fails if the leaves are under a water stressed situation. This result leads to the acceptance of the null hypothesis H03 and concludes that the determination of Chls using the chlorophyll meter (absorptance-based model) has a significant bias or uncertainty due to its failure of responding to the influence of water stress.

5 Conclusions

Typical vegetation reflectance is significantly related to foliar biochemistry and biophysical characteristics. A stronger negative relationship exists between the chlorophyll concentration and the visible reflectance while the relationship of the chlorophyll concentration and the infrared reflectance is positive. As water stress happened, the reflectance over the visible and infrared area will level up. The estimation of chlorophyll concentration using only the remotely sensed reflectance will be seriously affected by the reflectance changes caused by departure of water content from the fresh situation. The significant uncertainty for the estimation of chlorophyll concentration is caused by the reflectance changes induced by variations of the foliar water content. Red edge characteristics, such as position (λ_{REP}) and reflectance (ρ_{REP}) are also sensitive to water stress. Each of them, as a predictor of foliar Chls, has a significant positive linear relationship to foliar chlorophyll concentration. This is similar to the results of Matson et al. (1994) and Belanger et al. (1995).

The ChlsPn variables, such as the reflectance at the wavelengths 663, 645, 455, and 426 nm, are in particular directly related to the light absorption by chlorophyll *a* and chlorophyll *b* and therefore can characterize the foliar chlorophyll concentration. The relationship between Chls and each of the variables ρ_{426}, ρ_{455}, ρ_{645}, and ρ_{663} is statistically significant, but is still not good enough to be used alone for Chls estimation. The best adequacy (R^2) of the four reflectance-based ChlsPn models using one of the ChlsPn variables as the predictor is 0.77, meanwhile the best average accuracy achieved is MAE = 54 % and RMSE = 0.78 mg g^{-1} for both fresh and water stressed leaves. Spectral indices derived from ChlsPn variables by the methods of normalized difference, simple difference, slope transformation, and simple ratio can effectively improve the estimation accuracy of the reflectance-based Chls-spectral index models. The better accuracy is the model using the slope index SI_b with MAE = 17 % and RMSE = 0.44 mg g^{-1} or the difference index RDI_b with MAE = 18 % and RMSE = 0.46 mg g^{-1}. By integrating the reflectance at the red edge position, the difference-based simple ratio index $(\rho_{645} - \rho_{455})/\rho_{REP}$ can achieve the best accuracy of the Chls of fresh and water stressed leaves. The MAE and RMSE are further decreased down to 14 % and 0.36 mg g^{-1}, respectively.

Plant growth and productivity are mostly affected by water shortage. This stress condition induces plant cell dehydration and then causes the decreased chlorophylls in older leaves. Since the influence of water stress on foliar spectral reflectance could be effectively reduced by the reflectance at the red edge and the wavelength of 645, 455 nm, we recommend the following three spectral indices as effective chlorophyll indicator (ECI) for dealing with the potential influence of foliar water deficit for applications. The first predictor is the difference-based red edge reflectance ratio index ECI1 = $(\rho_{645} - \rho_{455})/\rho_{REP}$, then the slope index ECI2 = $(\rho_{645} - \rho_{455})/(\lambda_{645} - \lambda_{455})$, and finally the difference-based red edge position ratio index ECI3 = $(\rho_{645} - \rho_{455})/\lambda_{REP}$. ECI1 is negatively and linearly related to chlorophyll concentration, while ECI2 and ECI3 are exponential and negatively related to the natural-log transformed foliar chlorophyll concentration. A temporal and spatial estimation of the chlorophyll content for the

BGD
10, 17893–17937, 2013

terrestrial ecosystems could be retrieved more feasibly and accurately using these effective chlorophyll indicators.

References

Arnon, D. I.: Copper enzymes in isolated chloroplasts. Polyphenoloxidase in *Beta vulgaris*, Plant Physiol., 24, 1–15, 1949.

Blackburn, G. A.: Quantifying chlorophyll and caroteniods at leaf and canopy scales: an evaluation of some hyperspectral approaches, Remote Sens. Environ., 66, 273–285, 1998.

Blackburn, G. A.: Hyperspectral remote sensing of plant pigments, J. Exp. Bot., 58, 855–867, 2007.

Blackburn, G. A. and Ferwerda, J. G.: Retrieval of chlorophyll concentration from leaf reflectance spectra using wavelet analysis, Remote Sens. Environ., 112, 1614–1632, 2008.

Blackmer, T. M. and Schepers, J. S.: Use of a chlorophyll meter to monitor nitrogen status and schedule fertigation for corn, J. Prod. Agric., 8, 56–60, 1995.

Belanger, M. J., Miller, J. R., and Boyer, M. G.: Comparative relationships between some red edge parameters and seasonal leaf chlorophyll concentrations, Can. J. Remote Sens., 21, 16–21, 1995.

Boegh, E., Houborg, R., Bienkowski, J., Braban, C. F., Dalgaard, T., van Dijk, N., Dragosits, U., Holmes, E., Magliulo, V., Schelde, K., Di Tommasi, P., Vitale, L., Theobald, M. R., Cellier, P., and Sutton, M. A.: Remote sensing of LAI, chlorophyll and leaf nitrogen pools of crop- and grasslands in five European landscapes, Biogeosciences, 10, 6279–6307, doi:10.5194/bg-10-6279-2013, 2013.

Carter, G. A.: Primary and secondary effects of water content on the spectral reflectance of leaves, Am. J. Bot., 78, 916–924, 1991.

Carter, G. A.: Responses of leaf spectral reflectance to plant stress, Am. J. Bot., 80, 239–243, 1993.

Carter, G. A.: Ratios of leaf reflectances in narrow wavebands as indicators of plant stress, Int. J. Remote Sens., 15, 697–703, 1994.

Carter, G. A. and Knapp, A. K.: Leaf optical properties in higher plants, linking spectral characteristics to stress and chlorophyll concentration, Am. J. Bot., 88, 677–684, 2001.

BGD
10, 17893–17937, 2013

Cate, T. M. and Perkins, T. D.: Chlorophyll content monitoring in sugar maple (*Acer saccharum*), Tree Physiol., 23, 1077–1079, 2003.
Ceccato, P., Flasse, S., Tarantola, S., Jacquemoud, S., and Gregoire, J. M.: Detecting vegetation leaf water content using reflectance in the optical domain, Remote Sens. Environ., 77, 22–33, 2001.
Cheng, T., Rivard, B., and Sanchez-Azofeifa, A.: Spectroscopic determination of leaf water content using continuous wavelet analysis, Remote Sens. Environ., 115, 659–670, 2011.
Curran, P. J., Dungan, J. L., and Gholz, H. L.: Exploring the relationship between reflectance red edge and chlorophyll content in slash pine, Tree Physiol., 7, 33–48, 1990.
Curran, P. J., Dungan, J. L., Macler, B. A., and Plummer, S. E.: The effect of a red leaf pigment on the relationship between red edge and chlorophyll concentration, Remote Sens. Environ., 35, 69–76, 1991.
Curtiss, B. and Goetz, A. F. H.: Field Spectrometry: Techniques and Instrumentation, Proceedings of ISSSR 1994, 10–15 July, San Diego, California, 1, 195–203, 1994.
Dash, J. and Curran, P. J.: The MERIS terrestrial chlorophyll index, Int. J. Remote Sens., 25, 5403–5413, 2004.
Datt, B.: Remote sensing of chlorophyll *a*, chlorophyll *b*, chlorophyll $a+b$, and total carotenoid content in eucalyptus leaves, Remote Sens. Environ., 66, 111–121, 1998.
Daughtry, C. S. T., Walthall, C. L., Kim, M. S., de Colstoun, E. B., and McMurtrey III, J. E.: Estimating corn leaf chlorophyll concentration from leaf and canopy reflectance, Remote Sens. Environ., 74, 229–239, 2000.
Dawson, T. P., Curran, J. P., and Plummer, S. E.: LIBERTY – modeling the effects of leaf biochemical concentration on reflectance spectra, Remote Sens. Environ., 65, 50–60, 1998.
Desotgiu, R., Pollastrini, M., Cascio, C., Gerosa, G., Marzuoli, R., and Bussotti, F.: Chlorophyll *a* fluorescence analysis along a vertical gradient of the crown in a poplar (Oxford clone) subjected to ozone and water stress, Tree Physiol., 32, 976–986, 2012.
Elvidge, C. D. and Chen, Z.: Comparison of broad-band and narrow-band red and near-infrared vegetation indices, Remote Sens. Environ., 54, 38–48, 1995.
Emerson, R. and Lewis, C. M.: The dependence of the quantum yield of chlorella photosynthesis on wavelength of light, Am. J. Bot., 30, 165–178, 1943.
Estep, L. and Carter, G. A.: Derivative analysis of AVIRIS data for crop stress detection, Photogramm. Eng. Rem. S., 71, 1417–1421, 2005.

Féret, J. B., Francois, C., Gitelson, A., Asner, G. P., Barry, K. M., Panigada, C., Richardson, A. D., and Jacquemoud, S.: Optimizing spectral indices and chemometric analysis of leaf chemical properties using radiative transfer modeling, Remote Sens. Environ., 115, 2742–2750, 2011.

Filella, I. and Peñuelas, J.: The red edge position and shape as indicative plant chlorophyll content, biomass and hydric states, Int. J. Remote Sens., 15, 1459–1470, 1994.

Gausman, H. W. and Allen, W. A.: Optical parameters of leaves of 30 plant species, Plant Physiol., 52, 57–62, 1973.

Gausman, H. W., Escobar, D. E., and Rodriguez, R. R.: Reflectance measurements of cotton leaf senescence altered by mepiquat chloride, USDA/Agricultural Research Service, Remote Sensing Research Unit, Weslaco, Texas, 1982.

Ghorbanli, M., Gafarabad, M., Amirkian, T., and Allahverdi Mamaghani, B.: Investigation of proline, total protein, chlorophyll, ascorbate and dehydroascorbate changes under drought stress in Akria and Mobil tomato cultivars, Iran. J. Plant Physiol., 3, 651–658, 2013.

Gitelson, A. A. and Merzlyak, M. N.: Spectral reflectance changes associated with autumn senescence of *Aesculus hippocastanum* L., and *Acer platanoides* L. leaves. Spectral features and relation to chlorophyll estimation, J. Plant Physiol., 143, 286–292, 1994a.

Gitelson, A. A. and Merzlyak, M. N.: Quantitative estimation of chlorophyll *a* using reflectance spectra-experiments with autumn chestnut and maple leaves, J. Photoch. Photobio. B, 22, 247–252, 1994b.

Gitelson, A. A. and Merzlyak, M. N.: Signature analysis of leaf reflectance spectra: algorithm development for remote sensing of chlorophyll, J. Plant Physiol., 148, 494–500, 1996.

Gitelson, A. A. and Merzlyak, M. N.: Remote estimation of chlorophyll content in higher plant leaves, Int. J. Remote Sens., 18, 2691–2697, 1997.

Gitelson, A. A., Chivkunova, O. B., and Nerzlyak, M. N.: Nondestructive estimation of anthocyanins and chlorophylls in anthocyanic leaves, Am. J. Bot., 96, 1861–1868, 2009.

Gitelson, A. A., Gritz, U., and Merzlyak, M. N.: Relationships between leaf chlorophyll content and spectral reflectance and algorithms for non-destructive chlorophyll assessment in higher plant leaves, J. Plant Physiol., 160, 271–282, 2003.

Gitelson, A. A., Keydan, G. P., and Merzlyak, M. N.: Three-band model for noninvasive estimation of chlorophyll, carotenoids, and anthocyanin contents in higher plant leaves, Geophys. Res. Lett., 33, L11402, doi:10.1029/2006GL026457, 2006.

BGD
10, 17893–17937, 2013

Gond, V., de Pury, D. G. G., Veroustraete, F., and Ceulemans, R.: Seasonal variations in leaf area index, leaf chlorophyll, and water content; scaling-up to estimate fAPAR and carbon balance in a multilayer, multispecies temperate forest, Tree Physiol., 19, 673–679, 1999.

Haboudane, D., Tremblay, N., Miller, J. R., and Vigneault, P.: Remote estimation of crop chlorophyll content using spectral indices derived from hyperspectral data, IEEE T. Geosci. Remote, 46, 423–437, 2008.

Hatchell, D. C.: Analytical Spectral Devices, 4th edn., Technical Guide, ASD Inc, 1999.

Hawkins, T. S., Gardiner, E. S., and Comer, G. S.: Modeling the relationship between extractable chlorophyll and SPAD-502 readings for endangered plant species research, J. Nat. Conserv., 17, 125–129, 2009.

Horler, D. N. H., Dockray, M., and Barber, J.: The red edge of plant leaf reflectance, Int. J. Remote Sens., 4, 273–288, 1983.

Hopkins, W. G. and Hüner, N. P. A.: Introduction to Plant Physiology, 3rd edn., John Wiley & Sons, NJ, 2004.

Hunt, E. R. and Rock, B. N.: Detection of changes in leaf water content using near- and middle-infrared reflectances, Remote Sens. Environ., 30, 43–54, 1989.

Hunt, E. R., Daughtry, C. S. T., Eitel, J. U. H., and Long, D. S.: Remote sensing leaf chlorophyll content using a visible band index, Agron. J., 103, 1090–1099, 2011.

Hunt, E. R., Doraiswamy, P. C., McMurtrey, J. E., Daughtry, C. S. T., Perry, E. M., and Akhmedov, B.: A visible band index for remote sensing leaf chlorophyll content at the canopy scale, Int. J. Appl. Earth. Obs., 103, 1090–1099, 2013.

Jongschaap, R. E. E. and Booij, R.: Spectral measurements at different spatial scales in potato: relating leaf, plant and canopy nitrogen status, Int. J. Appl. Earth Obs., 5, 204–218, 2004.

Kaoau, M. E., Hsissou, D., and Belhadri, A.: Water deprivation effect on pigments and proline content, and growth in cultivated wheat varieties in Morocco, Afr. Crop Sci. J., 15, 139–147, 2007.

Keenan, T., García, R., Friend, A. D., Zaehle, S., Gracia, C., and Sabate, S.: Improved understanding of drought controls on seasonal variation in Mediterranean forest canopy CO_2 and water fluxes through combined in situ measurements and ecosystem modelling, Biogeosciences, 6, 1423–1444, doi:10.5194/bg-6-1423-2009, 2009.

Kirnak, H., Kaya, C., Tas, I., and Higgs, D.: The influence of water deficit on vegetative growth, physiology, fruit yield and quality in eggplants, Bulg. J. Plant Physiol., 27, 34–46, 2001.

Knipling, E. B.: Physical and physiological basis for the reflectance of visible and near-infrared radiation from vegetation, Remote Sens. Environ., 1, 155–159, 1970.
Lavoir, A.-V., Staudt, M., Schnitzler, J. P., Landais, D., Massol, F., Rocheteau, A., Rodriguez, R., Zimmer, I., and Rambal, S.: Drought reduced monoterpene emissions from the evergreen Mediterranean oak *Quercus ilex*: results from a throughfall displacement experiment, Biogeosciences, 6, 1167–1180, doi:10.5194/bg-6-1167-2009, 2009.
Lin, C., Tsogt, K., and Chang, C. I.: An empirical model-based method for signal restoration of SWIR in ASD field spectroradiometry, Photogramm. Eng. Rem. S., 78, 119–127, 2012.
Ma, B. L., Morrison, M. J., and Voldeng, H. D.: Leaf greenness and photosynthetic rates in soybean, Crop Sci., 35, 1411–1414, 1995.
Matson, P., Johnson, L., Billow, C., Miller, J., and Pu, R.: Seasonal patterns and remote spectral estimation of canopy chemistry across the Oregon transect, Ecol. Appl., 4, 280–298, 1994.
Montagu, K. D. and Woo, K. C.: Recovery of tree photosynthetic capacity from seasonal drought in the wet-dry tropicsw: the role of phyllode and canopy processes in *Acacia auriculiformis*, Aust. J. Plant Physiol., 26, 135–145, 1999.
Mutanga, O. and Skidmore, A. K.: Red edge shift and biochemical content in grass canopies, ISPRS J. Photogramm., 62, 34–42, 2007.
Nave, L. E., Gough, C. M., Maurer, K. D., Bohrer, G., Hardiman, B. S., Le Moine, J., Munoz, A. B., Nadelhoffer, K. J., Sparks, J. P., Strahm, B. D., Vogel, C. S., and Curtis, P. S.: Disturbance and the resilience of coupled carbon and nitrogen cycling in a north temperate forest, J. Geophys. Res., 116, G04016, doi:10.1029/2011JG001758, 2011.
Nilsen, E. T. and Orcutt, D. M.: Physiology of Plants Under Stress, Abiotic Factors, 2nd edn., John Wiley & Sons Inc., NY, 1996.
Nobel, P. S.: Physicochemical and Environmental Plant Physiology, 3rd edn., Academic Elsevier, Burlingtom, MA, 2005.
Oki, K.: Why is the ratio of reflectivity effective for chlorophyll estimation in the lake water?, Remote Sens., 2, 1722–1730, 2010.
Ollinger, S. V.: Sources of variability in canopy reflectance and the convergent properties of plants, New Phytol., 189, 375–394, 2011.
Pinar, A. and Curran, P. J.:, Grass chlorophyll and reflectance red edge, Int. J. Remote Sens., 17, 351–357, 1996.

BGD
10, 17893–17937, 2013

Pirzad, A., Shakiba, M. R., Zehtab-Salmasi, S., Mohammadi, S. A., Darvishzadeh, R., and Samadi, A.: Effect of water stress on leaf relative water content, chlorophyll, praline and soluble carbohydrates in *Matricaria chamomilla* L., J. Med. Plants Res., 5, 2483–2488, 2011.

Pu, R., Ge, S., Kelly, N. M., and Gong, P.: Spectral absorption features as indicators of water status in coast live oak (*Quercus agrifolia*) leaves, Int. J. Remote Sens., 24, 1799–1810, 2003.

Rascher, U., Agati, G., Alonso, L., Cecchi, G., Champagne, S., Colombo, R., Damm, A., Daumard, F., de Miguel, E., Fernandez, G., Franch, B., Franke, J., Gerbig, C., Gioli, B., Gómez, J. A., Goulas, Y., Guanter, L., Gutiérrez-de-la-Cámara, Ó., Hamdi, K., Hostert, P., Jiménez, M., Kosvancova, M., Lognoli, D., Meroni, M., Miglietta, F., Moersch, A., Moreno, J., Moya, I., Neininger, B., Okujeni, A., Ounis, A., Palombi, L., Raimondi, V., Schickling, A., Sobrino, J. A., Stellmes, M., Toci, G., Toscano, P., Udelhoven, T., van der Linden, S., and Zaldei, A.: CEFLES2: the remote sensing component to quantify photosynthetic efficiency from the leaf to the region by measuring sun-induced fluorescence in the oxygen absorption bands, Biogeosciences, 6, 1181–1198, doi:10.5194/bg-6-1181-2009, 2009.

Read, J. J., Whaley, E. L., Tarpley, L., and Reddy, R.: Evaluation of a hand-held radiometer for field determination of nitrogen status in cotton, in: Digital Imaging and Spectral Techniques: Applications to Precision Agriculture and Crop Physiology, edited by: Schepers, J. and von Toai, T., ASA, Madison, Wis, 171–189, 2003.

Reddy, K. R. and Matcha, S. K.: Remote sensing algorithms for castor bean nitrogen and pigment assessment for fertility management, Ind. Crop. Prod., 32, 411–419, 2010.

Rossini, M., Cogliati, S., Meroni, M., Migliavacca, M., Galvagno, M., Busetto, L., Cremonese, E., Julitta, T., Siniscalco, C., Morra di Cella, U., and Colombo, R.: Remote sensing-based estimation of gross primary production in a subalpine grassland, Biogeosciences, 9, 2565–2584, doi:10.5194/bg-9-2565-2012, 2012.

Rowland, D., Blankenship, P., Puppala, N., Beasley, J., Burow, M., Gorbet, D., Jordan, D., Melouk, H., Simpson, C., and Bostick, J.: Variation in water-use efficiency of peanut varieties across peanut production regions, http://www.cropscience.org.au/icsc2004/poster/1/3/2/288_rowlanddl.htm (last access: 10 November 2012), 2004.

Schelbert, S., Aubry, S., Burla, B., Agne, B., Kessler, F., Krupinska, K., and Hörtensteiner, S.: Pheophytin pheophorbide hydrolase (pheophytinase) is involved in chlorophyll breakdown during leaf senescence in *Arabidopsis*, Plant Cell, 21, 767–785, 2009.

Sims, D. A. and Gamon, J. A.: Relationships between leaf pigment content and spectral reflectance across a wide range of species, leaf structures and development stages, Remote Sens. Environ., 81, 337–354, 2002.
Takebe, M., Yoneyama, T., Inada, K., and Murakami, T.: Spectral reflectance ratio of rice canopy for estimating crop nitrogen status, Plant Soil, 122, 295–297, 1990.
Tan, S. C., Shi, G. Y., Shi, J. H., Gao, H. W., and Yao, X.: Correlation of Asian dust with chlorophyll and primary productivity in the coastal seas of China during the period from 1998 to 2008, J. Geophys. Res., 116, G02029, doi:10.1029/2010JG001456, 2011.
Ustin, S. L., Gitelson, A. A., Jacquemoud, S., Schaepman, M., Asner, G. P., Gamon, J. A., and Zarco-Tejada, P.: Retrieval of foliar information about plant pigment systems from high resolution spectroscopy, Remote Sens. Environ., 113, S67–S77, 2009.
Vogelmann, J. E., Rock, B. N., and Moss, D. M.: Red edge spectral measurements from sugar maple leaves, Int. J. Remote Sens., 14, 1563–1575, 1993.
Weber, U., Jung, M., Reichstein, M., Beer, C., Braakhekke, M. C., Lehsten, V., Ghent, D., Kaduk, J., Viovy, N., Ciais, P., Gobron, N., and Rödenbeck, C.: The interannual variability of Africa's ecosystem productivity: a multi-model analysis, Biogeosciences, 6, 285–295, doi:10.5194/bg-6-285-2009, 2009.
Wellburn, A. R.: The spectral determination of chlorophylls *a* and *b*, as well as total carotenoids, using various solvents with spectrophotometers of different resolution, J. Plant Physiol., 144, 307–313, 1994.
Whittaker, R. H. and Marks, P. L.: Methods of assessing terrestrial productivity, in: Primary Productivity of the Biosphere, edited by: Lieth, H. and Whittaker, R. H., Springer-Verlag, NY, 55–118, 1975.
Wuyts, N., Massonnet, C., Dauzat, M., and Granier, C.: Structural assessment of the impact of environmental constraints on *Arabidopsis thaliana* leaf growth: a 3-D approach, Plant Cell Environ., 35, 1631–1646, 2012.
Zygielbaum, A. I., Gitelson, A. A., Arkebauer, T. J., and Rundquist, D. C.: Non-destructive detection of water stress and estimation of relative water content in maize, Geophys. Res. Lett., 36, L12403, doi:10.1029/2009GL038906, 2009.

BGD
10, 17893–17937, 2013

Table 1. Previously developed spectral indices for foliar chlorophyll estimation.

Index	Formula	Source
Vogelmann red edge index 1	$\text{Vog1} = \rho_{740}/\rho_{720}$	Vogelmann et al. (1993)
Vogelmann red edge index 2	$\text{Vog2} = (\rho_{734} - \rho_{747})/(\rho_{715} + \rho_{726})$	Vogelmann et al. (1993)
Vogelmann red edge index 3	$\text{Vog3} = (\rho_{734} - \rho_{747})/(\rho_{715} + \rho_{720})$	Vogelmann et al. (1993)
Red-edge NDVI	$\text{NDVI}_{705} = (\rho_{750} - \rho_{705})/(\rho_{750} + \rho_{705})$	Gitelson and Merzlyak (1994a, b)
Normalized difference vegetation index	$\text{NDVI}_{700} = (\rho_{800} - \rho_{700})/(\rho_{800} + \rho_{700})$	Gitelson and Merzlyak (1994a, b)
Simple ratio index	$\text{SR}_{700} = \rho_{750}/\rho_{700}$	Gitelson and Merzlyak (1996, 1997), Boegh et al. (2012)
Weighted simple ratio	$\text{wSR} = \rho_{860}/(\rho_{708} \times \rho_{550})$	Datt (1998), Gitelson et al. (2003)
Normalized difference vegetation index	$\text{NDVI}_{680} = (\rho_{800} - \rho_{680})/(\rho_{800} + \rho_{680})$	Blackburn (1998)
Modified chlorophyll absorption reflectance index	$\text{MCARI} = [(\rho_{700} - \rho_{670}) - 0.2(\rho_{700} - \rho_{550})][\rho_{700}/\rho_{670}]$	Daughtry et al. (2000)
Modified red-edge simple ratio	$\text{mSR} = (\rho_{750} - \rho_{445})/(\rho_{705} - \rho_{445})$	Sims and Gamon (2002)
Modified red-edge NDVI	$\text{mNDVI} = (\rho_{750} - \rho_{705})/(\rho_{750} + \rho_{705} - 2\rho_{445})$	Sims and Gamon (2002)
MERIS total chlorophyll index	$\text{MTCI} = (\rho_{750} - \rho_{710})/(\rho_{710} - \rho_{680})$	Dash and Curran (2004), Rossini et al. (2012)
Reciprocal-based simple ratio index	$\text{rSR}_{705} = \left(\frac{1}{\rho_{705}} - \frac{1}{\rho_{780}}\right) \times \rho_{780} = (\rho_{780}/\rho_{705}) - 1$	Gitelson et al. (2006)
Triangular chlorophyll index	$\text{TCI} = 1.2(\rho_{700} - \rho_{550}) - 1.5(\rho_{670} - \rho_{550})(\rho_{700}/\rho_{670})^{0.5}$	Haboudane et al. (2008)
Simple ratio index	$\text{SR}_{775} = \rho_{708}/\rho_{775}$	Féret et al. (2011)
Normalized difference vegetation index	$\text{NDVI}_{712} = (\rho_{780} - \rho_{712})/(\rho_{780} + \rho_{712})$	Féret et al. (2011)
Triangular greenness index	$\text{TGI} = -0.5[190(\rho_{670} - \rho_{550}) - 120(\rho_{670} - \rho_{480})]$	Hunt et al. (2011, 2013)
Simple ratio stress index	$\text{SR}_{760} = \rho_{695}/\rho_{760}$	Carter (1994)
Simple ratio stress index	$\text{SR}_{420} = \rho_{695}/\rho_{420}$	Carter (1994)
Simple ratio index broadband red edge	$\text{CI}_{\text{red edge}} = (\rho_{760\text{–}800}/\rho_{690\text{–}710}) - 1$	Gitelson et al. (2009)

BGD
10, 17893–17937, 2013

Table 2. The meaning and the formula of some extended spectral indices derived from the ChlsPn variables, red edge and green peak variables.

Regressor names	Meaning and mathematical formula	
RDI group	Reflectance Difference Index of two spectral features from ChlsPN, red edge, and green peak.	
RDI_a	RDI derived based on the two absorption peaks of chlorophyll *a* at 663 nm and 426 nm. $RDI_a = \rho_{663} - \rho_{426}$	(6)
RDI_b	RDI derived based on the two absorption peaks of chlorophyll *b* at 645 nm and 455 nm. $RDI_b = \rho_{645} - \rho_{455}$	(7)
$RDI_{\rho_{REP}-\rho_{Gmax}}$	RDI derived based on the red edge and green peak position. $RDI_{\rho_{REP}-\rho_{Gmax}} = \rho_{REP} - \rho_{Gmax}$	(8)
SI group	Slope index of two spectral features from ChlsPN, red edge, and green peak.	
SI_a	SI determined using the two absorption peaks of chlorophyll *a*. $SI_a = (\rho_{663} - \rho_{426})/(\lambda_{663} - \lambda_{426})$	(9)
SI_b	SI determined using the two absorption peaks of chlorophyll *b*. $SI_b = (\rho_{645} - \rho_{455})/(\lambda_{645} - \lambda_{455})$	(10)
$SI_{\rho_{REP}\vert\rho_{Gmax}}$	SI determined using the red edge and green peak features. $SI_{\rho_{REP}\vert\rho_{Gmax}} = (\rho_{REP} - \rho_{Gmax})/(\lambda_{REP} - \lambda_{Gmax})$	(11)
NDI group	Normalized Difference Index of two spectral features from ChlsPN, red edge, and green peak.	
NDI_a	$NDI_a = (\rho_{663} - \rho_{426})/(\rho_{663} + \rho_{426})$	(12)
NDI_b	$NDI_b = (\rho_{645} - \rho_{455})/(\rho_{645} + \rho_{455})$	(13)
$NDI_{REPRDIb}$	$NDI_{REPRDIb} = (\rho_{REP} - RDI_b)/(\rho_{REP} + RDI_b)$	(14)
$NDI_{REPGmax}$	$NDI_{REPGmax} = (\rho_{REP} - \rho_{Gmax})/(\rho_{REP} + \rho_{Gmax})$	(15)
RI group	Ratio Index of two spectral features from ChlsPN, red edge, and green peak.	
RI_a	$RI_a = \rho_{663}/\rho_{426}$	(16)
RI_b	$RI_b = \rho_{645}/\rho_{455}$	(17)
$RI_{RDI_b/\rho_{REP}}$	$RI_{RDI_b/\rho_{REP}} = RDI_b/\rho_{REP}$	(18)
$RI_{RDI_b/\lambda_{REP}}$	$RI_{RDI_b/\lambda_{REP}} = RDI_b/\lambda_{REP}$	(19)
$RI_{\rho_{Gmax}/\rho_{REP}}$	$RI_{\rho_{Gmax}/\rho_{REP}} = \rho_{Gmax}/\rho_{REP}$	(20)
RI_{SPAD}	$RI_{SPAD} = \rho_{650}/\rho_{940}$	(21)

BGD
10, 17893–17937, 2013

Effective chlorophyll indicators for fresh and water-stressed leaves

C. Lin et al.

Title Page
Abstract | Introduction
Conclusions | References
Tables | Figures
Back | Close
Full Screen / Esc
Printer-friendly Version
Interactive Discussion

Table 3. Prediction accuracy assessment of the developed Chls empirical models.

Predictor	Model adequacy			Model validation					
	R^2	PRESS	SE(Y)	RMSEf	RMSEw	RMSEa	MAEf	MAEw	MAEa
$RI_{RDI_b/\rho_{REP}}$	0.90	1.55	0.17	0.35	0.38	0.36	15.85	12.49	14.17
SI_b	0.94	0.93	0.13	0.46	0.43	0.44	19.07	14.63	16.85
$RI_{RDI_b/\lambda_{REP}}$	0.94	0.93	0.13	0.46	0.42	0.44	19.33	14.47	16.90
RDI_b	0.94	0.93	0.13	0.44	0.49	0.46	17.11	18.03	17.57
$NDI_{REPRDIb}$	0.92	1.30	0.16	0.36	0.48	0.43	16.78	18.97	17.88
ρ_{REP}	0.30	10.97	0.46	0.52	0.44	0.48	20.45	20.79	20.62
NDI_b	0.84	2.49	0.22	0.40	0.55	0.48	21.11	24.36	22.74
RI_b	0.83	2.70	0.23	0.39	0.54	0.47	21.49	24.01	22.75
NDI_a	0.68	5.08	0.31	0.73	0.67	0.70	32.83	31.12	31.98
RI_a	0.66	5.36	0.32	0.64	0.70	0.67	32.05	33.05	32.55
SI_a	0.87	2.00	0.20	0.85	0.54	0.71	50.56	20.47	35.51
RDI_a	0.74	9.98	0.44	0.85	0.54	0.71	50.56	20.47	35.51
RI_{SPAD}	0.79	3.41	0.25	0.79	0.49	0.66	48.04	36.20	42.12
$RDI_{\rho_{REP}-\rho_{Gmax}}$	0.92	1.25	0.15	1.20	0.78	1.01	55.63	39.73	47.68
$SI_{\rho_{REP}\vert\rho_{Gmax}}$	0.92	1.25	0.25	1.15	0.78	0.98	54.55	39.34	49.95
λ_{REP}	0.90	1.59	0.18	1.18	0.64	0.95	56.05	48.43	52.24
$RI_{\rho_{Gmax}/\rho_{REP}}$	0.93	1.06	0.14	0.40	1.17	0.88	16.33	89.52	52.93
ρ_{645}	0.77	3.57	0.26	0.98	0.63	0.82	60.38	46.41	53.39
$NDI_{REPGmax}$	0.93	1.08	0.14	0.40	1.19	0.89	16.49	90.71	53.60
ρ_{426}	0.19	12.63	0.50	0.84	0.72	0.78	54.73	54.99	54.86
ρ_{663}	0.55	6.99	0.37	1.12	0.60	0.90	70.54	43.91	57.23
ρ_{455}	0.27	11.29	0.47	1.02	0.85	0.94	66.31	64.24	65.28
ρ_{Gmax}	0.92	1.19	0.15	0.78	1.94	1.48	44.61	147.80	96.20
λ_{Gmax}	0.10	14.09	0.52	0.90	> 1000	> 1000	57.00	> 1000	> 1000

Table 4. Narrow-band-based spectral indices developed as chlorophyll indicators.

Indicator	Chls estimation models (y is lnChls)	R^2	PRESS	SE(Y)
Vog1	$y = -4.0302 + 3.4801\,\mathrm{Vog1}$	0.94	0.95	0.13
Vog2	$y = -0.4049 - 19.4238\,\mathrm{Vog2}$	0.94	0.95	0.13
Vog3	$y = -0.3766 - 17.3277\,\mathrm{Vog3}$	0.94	0.94	0.13
NDVI_{705}	$y = -0.8710 + 3.6844\,\mathrm{NDVI}_{705}$	0.92	1.21	0.15
NDVI_{700}	$y = -1.0487 + 3.1896\,\mathrm{NDVI}_{700}$	0.91	1.46	0.17
SR_{700}	$y = -0.8609 + 0.4175\,\mathrm{SR}_{700}$	0.94	1.00	0.14
wSR	$y = -0.3406 + 5.5226\,\mathrm{wSR}$	0.91	1.47	0.17
NDVI_{680}	$y = -5.5313 + 7.5436\,\mathrm{NDVI}_{680}$	0.60	6.29	0.35
MCARI	$y = 1.3432 - 0.0192\,\mathrm{MCARI}$	0.82	2.86	0.24
mSR	$y = -0.9494 + 0.5288\,\mathrm{mSR}$	0.94	0.91	0.13
mNDVI	$y = -0.8980 + 3.2961\,\mathrm{mNDVI}$	0.92	1.31	0.16
MTCI	$y = -0.4718 + 0.9146\,\mathrm{MTCI}$	0.94	1.01	0.14
rSR_{705}	$y = -0.4432 + 0.6887\,\mathrm{rSR}_{705}$	0.94	0.91	0.13
TCI	$y = 3.7126 \cdot \exp(-0.0743\,\mathrm{TCI})$	0.88	1.94	0.19
SR_{775}	$y = 22.5416 \cdot \exp(-8.1018\,\mathrm{SR}_{775})$	0.90	1.56	0.17
NDVI_{712}	$y = -0.6772 + 4.7009\,\mathrm{NDVI}_{712}$	0.93	1.15	0.15
TGI	$y = 1.7411 - 0.0011\,\mathrm{TGI}$	0.93	1.11	0.15
SR_{760}	$y = -0.3563 + 3.4783 \cdot \exp(-6.6687\,\mathrm{SR}_{760})$	0.91	1.50	0.17
SR_{420}	$y = 1.8611 - 0.4905\,\mathrm{SR}_{420}$	0.66	5.24	0.32
$\mathrm{CI}_{\text{red edge}}$	$y = -0.5205 + 0.4737\,\mathrm{CI}_{\text{red edge}}$	0.93	1.05	0.14

BGD
10, 17893–17937, 2013

Table 5. Foliar Chls prediction accuracy of the previously developed spectral indices.

Error index / Chls indicator	RMSE ($mg\,g^{-1}$) Fresh sample	Wilted sample	All	MAE (%) Fresh sample	Wilted sample	All
Vog1	1.91	0.33	1.37	78.35	13.96	46.15
Vog2	3.01	0.41	2.15	111.33	27.99	69.66
Vog3	3.27	0.39	2.33	115.85	25.78	70.81
$NDVI_{705}$	1.43	0.54	1.08	78.32	39.56	58.94
$NDVI_{700}$	1.36	0.86	1.14	82.51	63.74	73.12
SR_{700}	4.28	0.48	3.04	155.11	34.37	94.74
wSR	3.65	2.49	3.12	93.48	170.68	132.08
$NDVI_{680}$	1.27	0.47	0.95	78.15	32.27	55.21
MCARI	1.06	1.55	1.33	71.17	119.34	95.26
mSR	6.44	0.41	4.57	173.85	28.68	101.26
mNDVI	1.46	0.57	1.11	78.08	42.21	60.14
MTCI	2.80	0.34	1.99	95.57	22.05	58.81
rSR_{705}	3.62	0.54	2.59	129.23	39.78	84.50
TCI	2.67	3.67	3.21	85.89	268.02	176.95
SR_{775}	5.98	0.38	4.24	171.87	26.43	99.15
$NDVI_{712}$	1.49	0.54	1.12	72.86	40.55	56.71
TGI	0.57	2.33	1.70	30.13	178.95	104.54
SR_{760}	1.93	0.54	1.41	102.96	38.92	70.94
SR_{420}	0.99	0.83	0.92	63.28	61.48	62.38
$CI_{\text{broad band}}$	0.71	1.00	0.87	27.10	51.86	39.48

BGD
10, 17893–17937, 2013

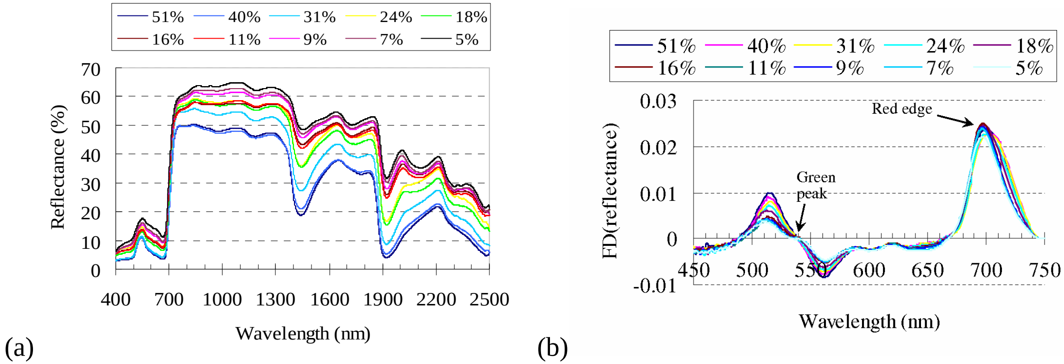

Fig. 1. Foliar reflectance spectra of *Cinnamomum canphora*. **(a)** Spectral curves showed the reflectance variation of visible-infrared bands due to the changes of water content. **(b)** An example of the association between the relative water content in fresh and water-stressed leaves and the green peak and red edge spectra features.

BGD
10, 17893–17937, 2013

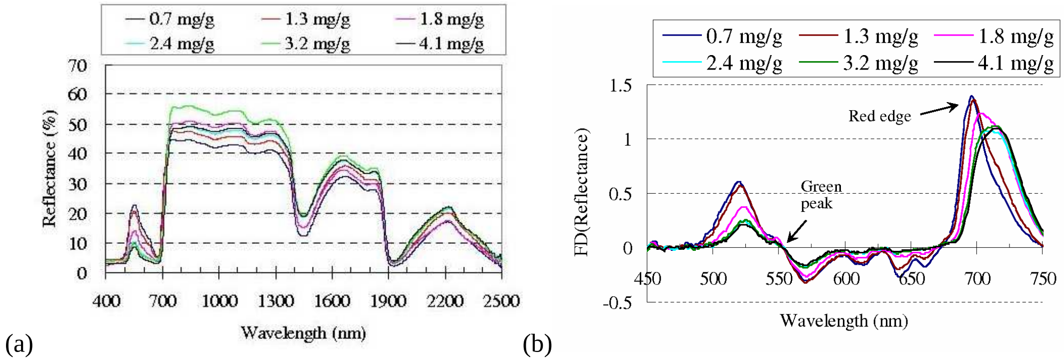

Fig. 2. Foliar reflectance spectra of *Cinnamomum canphora*. **(a)** Spectral curves showed the reflectance variation of visible-infrared bands due to the changes of foliar chlorophylls concentration. **(b)** Association between the chlorophylls concentration and the green peak and red edge spectra of fresh leaves.

BGD
10, 17893–17937, 2013

Effective chlorophyll indicators for fresh and water-stressed leaves

C. Lin et al.

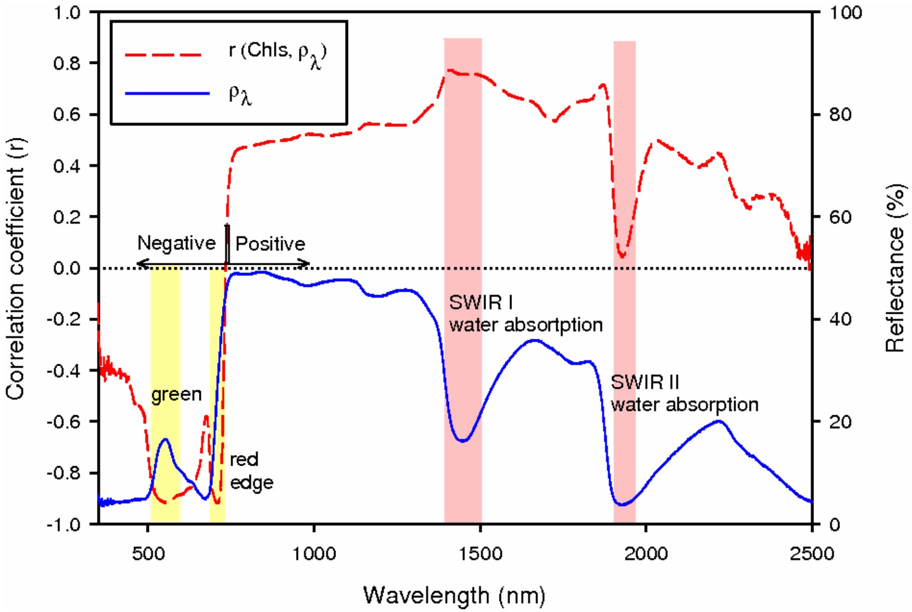

Fig. 3. Generalized reflectance spectra of *Cinnamomum camphora* leaf (solid line) and trends of the corresponding correlation coefficients (dashed line) between the concentration of total chlorophylls and reflectance in the visible-infrared wavelength region. Results derived from the training data set, the 50 leaf samples.

BGD
10, 17893–17937, 2013

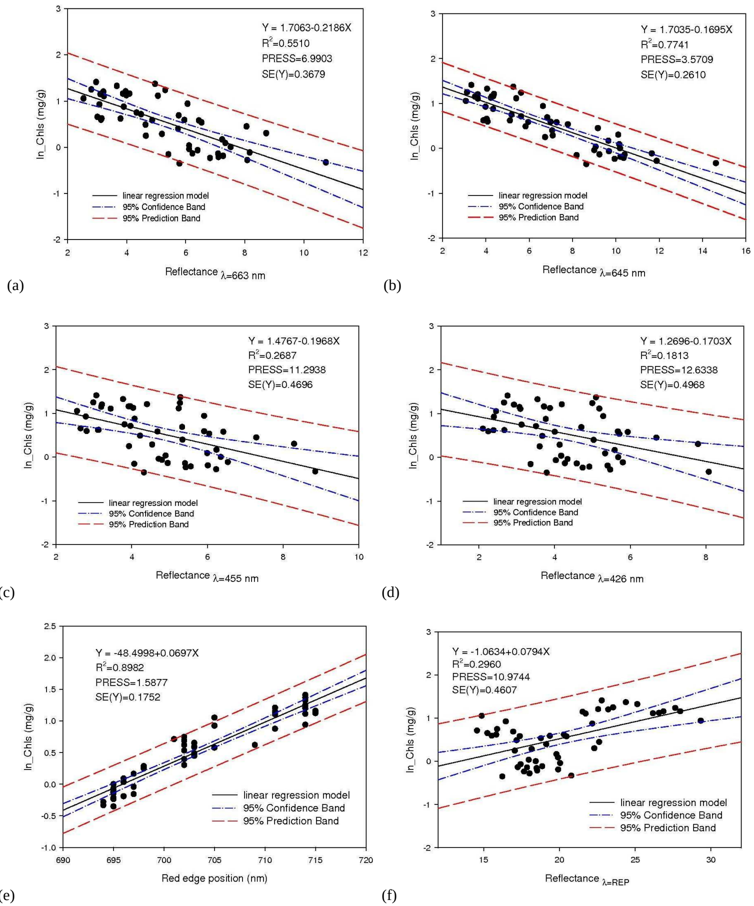

Fig. 4. Reflectance based empirical models with the ChlsPn/red edge/green peak variables for leaf total chlorophyll content estimation.

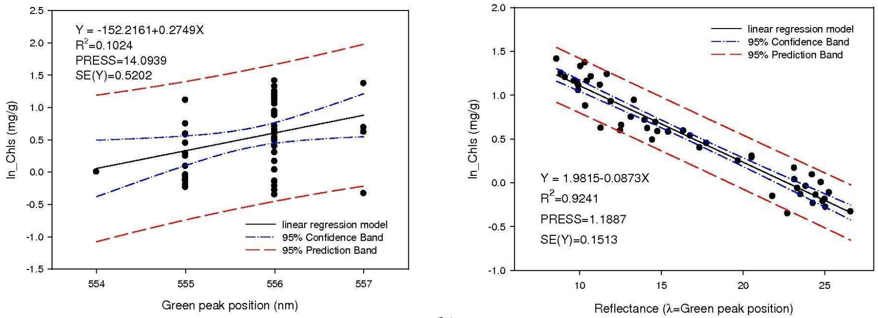

(g) (h)

Fig. 4. Continued.

BGD

10, 17893–17937, 2013

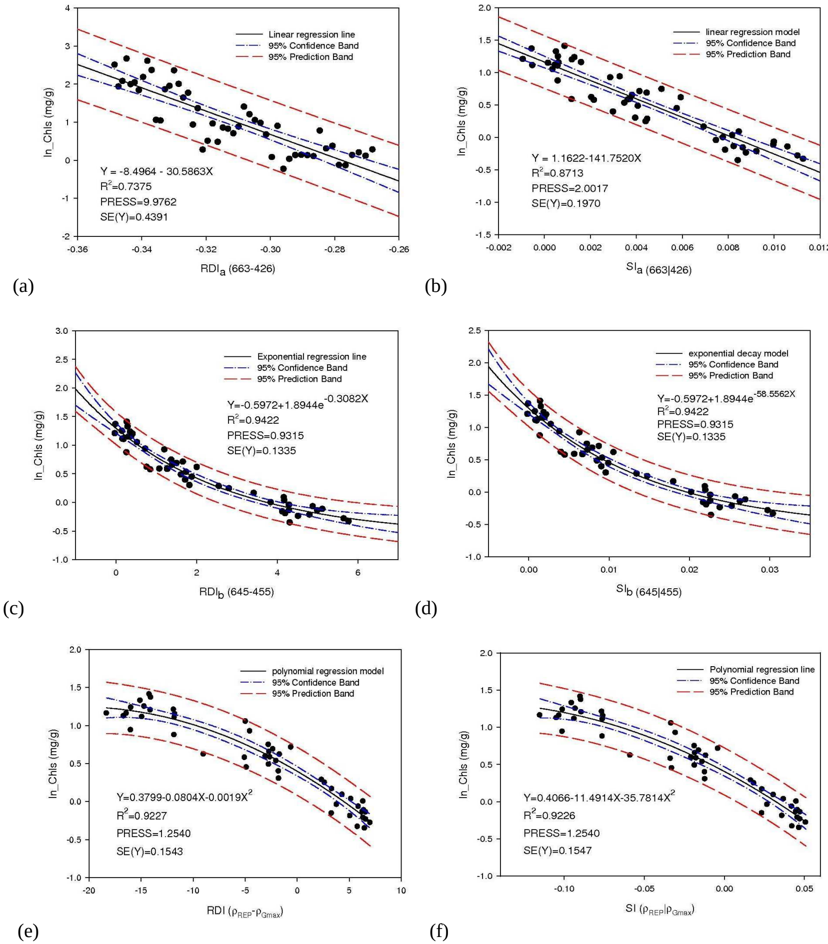

Fig. 5. RDIs and SIs based empirical models for the estimation of foliar total chlorophyll concentration.

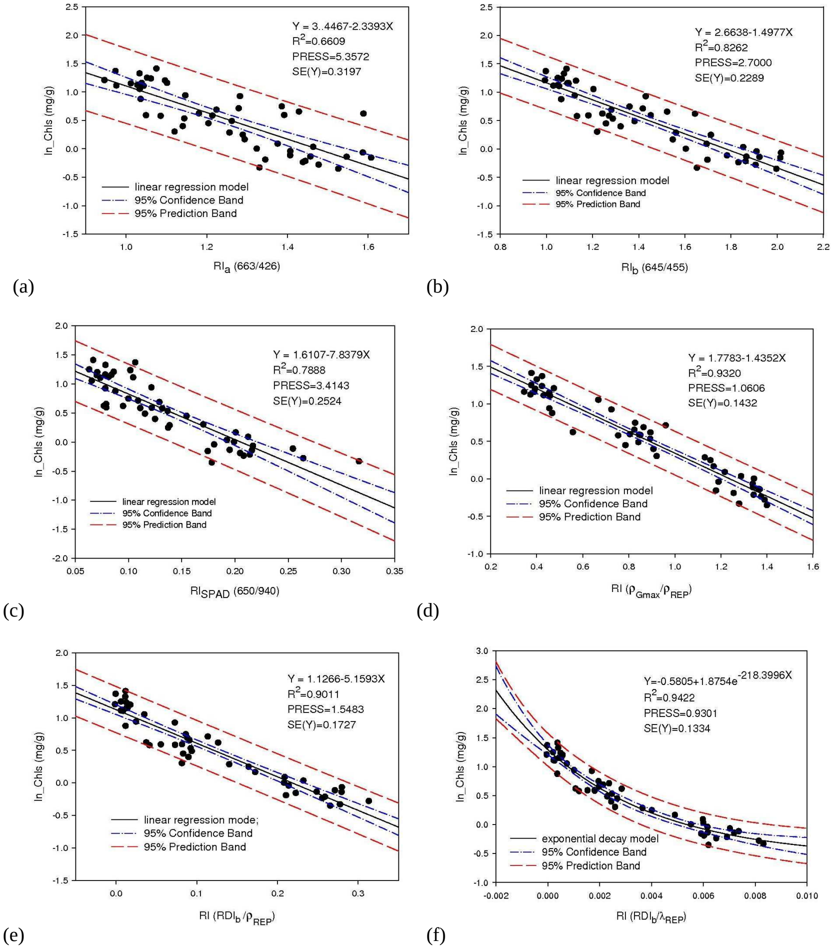

Fig. 6. Ratio index based empirical models for foliar chlorophylls concentration estimation.

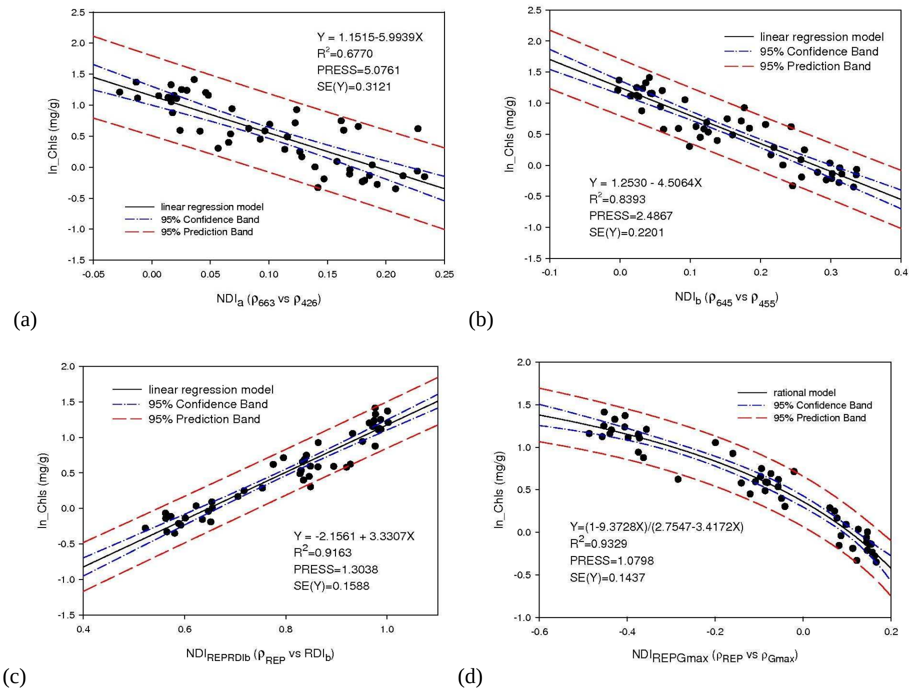

Fig. 7. Normalized difference index based empirical models for foliar chlorophylls concentration estimation.

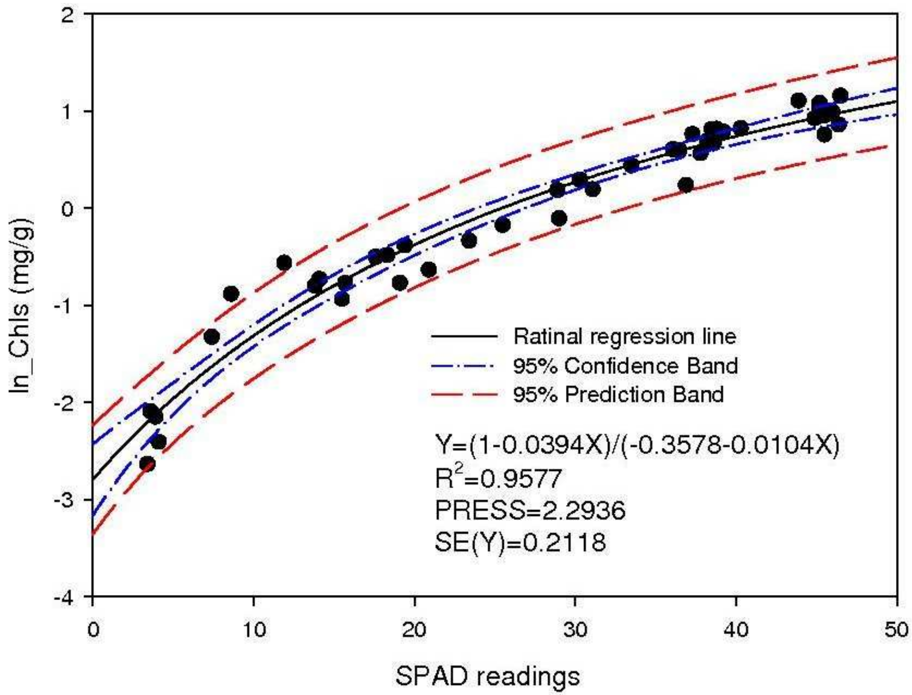

Fig. 8. Rational regression model for foliar chlorophyll contents estimation. Number of data points is 45. In the rational model, the independent variable SPAD-reading could be used to explain 95.77 % (R^2) variation of the dependent variable, lnChls, the natural logarithm transformed foliar chlorophylls contents.

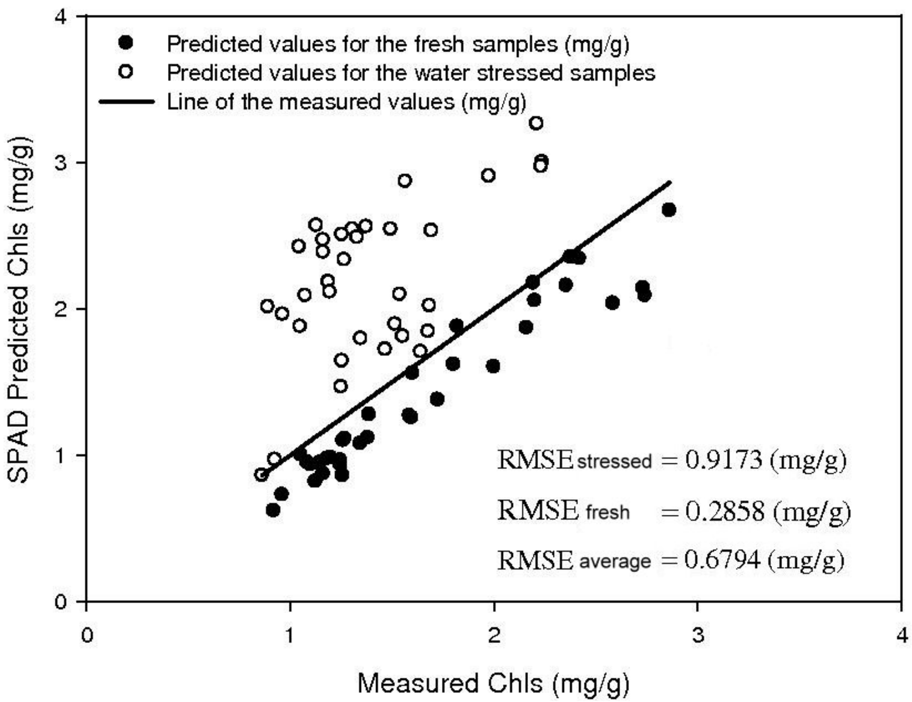

Fig. 9. Evaluation of the prediction accuracy of the SPAD-Chlorophyll regression model. Number of data points = 70. For the testing fresh samples, the estimation error is 0.2858 mg g^{-1}; for the testing samples which are water stressed, the error is 0.9173 mg g^{-1}. Average error is 0.6794 mg g^{-1} for all of the testing data points.

BGD
10, 17893–17937, 2013